Supplementary Material: Evanescent-Field Assisted Photon Collection from Quantum Emitters under a Solid Immersion Lens

S.G. Bishop,[†] J.K. Cannon,[†] H.B. Yağcı,[†] R.N. Clark,[†] J.P. Hadden,[†] W.W. Langbein,[‡] and A.J. Bennett[*,†,‡]

[†]*School of Engineering, Cardiff University, Queen's Building, The Parade, Cardiff, UK, CF24 3AA*

[‡]*School of Physics and Astronomy, Cardiff University, Queen's Building, The Parade, Cardiff, UK, CF24 3AA*

E-mail: BennettA19@cardiff.ac.uk

Sample Configuration

The AlN samples used for the investigation are taken from the same 2 inch c-plane AlN-on-sapphire wafer commercially purchased from Dowa Electronics Materials Co., Ltd. The AlN epilayer, grown on a c-plane sapphire substrate, is specified with a thickness of 1 µm with a variation across the wafer of 2.3 %. Tapping mode atomic force microscopy measurements, taken from the manufactures datasheet, reveals an average surface roughness of 2.5 Å. X-ray rocking curve measurements on the (0002) plane revealed a full width at half maximum of 47 arcsec.

Laser Scanning Confocal Microscope

All optical measurements presented in this work are taken on a room temperature laser scanning confocal microscope (LSCM) optimised for diffraction limited imaging across the visible spectrum. An illustration of the microscope can be observed in Fig.SM1. A 532 nm continuous wave frequency-doubled Nd:YAG is coupled into single mode fiber (SMF) using mirrors M7 and M8 via the achromatic lens L7. The Faraday rotator FR and linear polariser LP2 avoid back reflections into the laser cavity. The excitation laser is coupled into the microscope using the achromatic lens L1 from the SMF. The excitation is focused onto the sample using a Zeiss microscope objective with a numerical aperture (NA) of 0.9. The collected fluorescence is split from the excitation using the dichroic mirror BS1, which has a cut-on wavelength of 550 nm. Optical long and short pass filters, represented by F2 in the figure, limit the measurement of fluorescence within the 550 to 650 nm optical window. No further optical filtering is used for any of the measurements within the report, including the second order correlation measurements. The excitation and collection beam paths are spatially overlapped using the mirrors M1, M4 and M5. The diffraction limited excitation is scanned across the sample using a 4f relay system. M2 is a dual-axis galvanometric scanning mirror. The change in optical angle $\Delta\theta$ of the achromatic lens L2 is translated to a change of displacement ΔD on the sample surface using the simple geometric expression $\Delta D = f_e \tan(\Delta\theta)$ for identical lenses L2 and L3, where f_e is the effective focal length of the microscope objective MO. Using the high NA objective,

emitters are imaged with a FWHM resolution in the order of 450 nm.

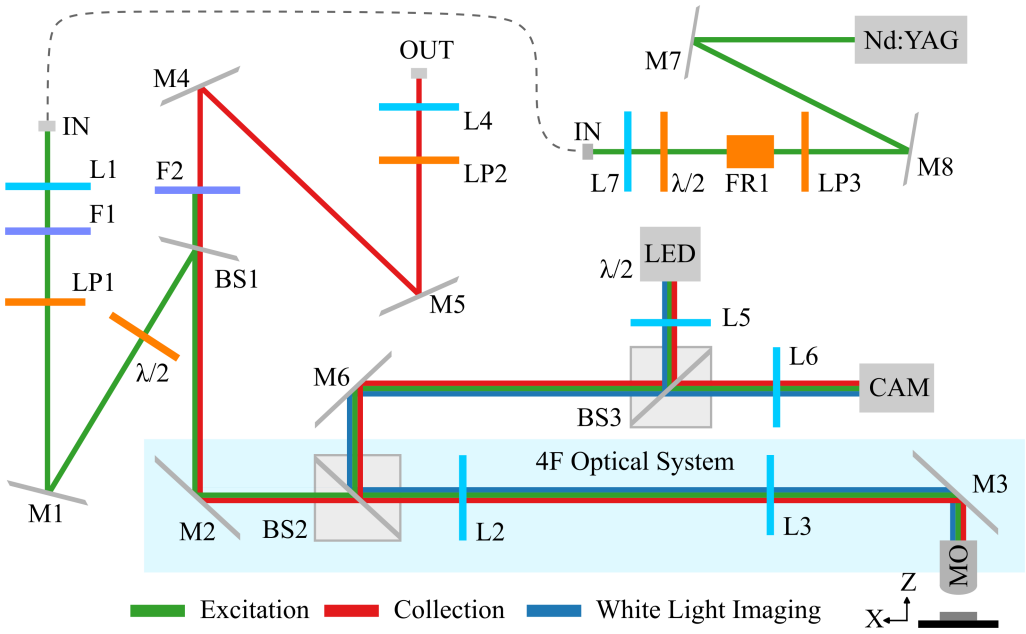

Figure 1: Illustration of the room temperature laser scanning confocal microscope. The laser excitation and collection is coupled into and out of the microscope into single mode optical fibre. The components are as follows: Lx - achromatic lens, Fx - optical filter, Mx - mirror, BSx - beam splitter, LPx - linear polariser, $\lambda/2$ - half-wave plate, FR - Faraday rotator and MO - microscope objective.

The collected fluorescence from the sample is coupled into SMF using the achromatic lens L4 and measured on a single photon sensitive avalanche diode (SPAD). The silicon SPAD is sensitive to photons across the visible spectrum, with a photon detection efficiency of 65 % at 650 nm and 45 % at 850 nm. A second SPAD is used for auto-correlation measurements, where an in-fiber 50 : 50 beamsplitter is used to split the photons between the two detection channels. Photon arrival times are recorded for each channel using time correlated single photon counting (TCSPC) electronics. The second order correlation data is obtained by post-processing the photon arrival times. Polarisation resolved absorption measurements are enabled using the linear polariser LP1 and an achromatic half-wave plate $\lambda/2$.

Second Order Correlation Fitting

The second order correlation measurements were fit with the following function[1];

$$g^{(2)}(\tau) = (1-(1+\beta)e^{\frac{-|t-t_0|}{\tau_1}} + \beta e^{\frac{-|t-t_0|}{\tau_2}}) \quad \text{(SM1)}$$

where β is the bunching ratio, t_0 is a time offset in the x-axis, τ_1 is the antibunching lifetime and τ_2 is the bunching lifetime.

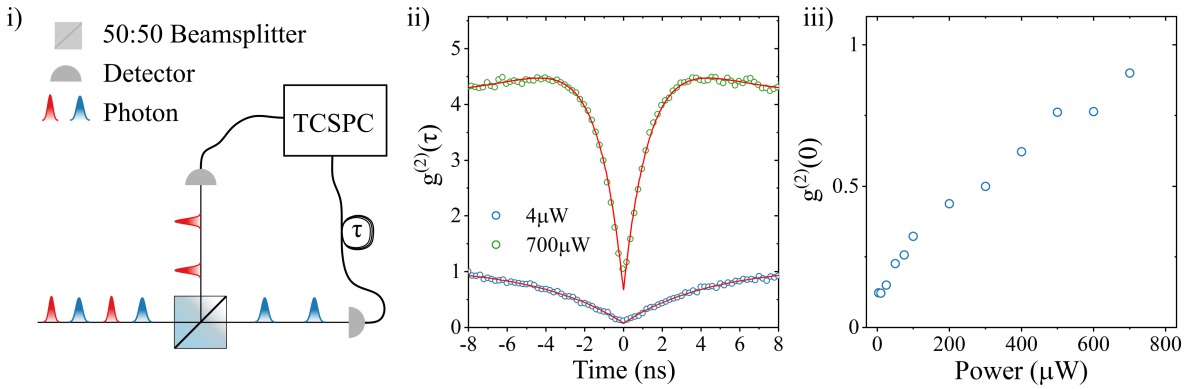

Figure 2: Second order correlation. i) Illustration of the Hanbury Brown & Twiss interferometer used to measure the second order correlation of the light from the emitters. ii) Low (4 μW) and high (700 μW) second order correlation measurements fit with the function in Eq.SM1. iii) $g^{(2)}$ value at time zero for each power dependent second order correlation measurement.

An illustration of the Hanbury Brown & Twiss (HBT) interferometer used to measure the second order correlation of the light from the emitters is shown in Fig.2.(i). The photon stream from the emitter is split by a 50:50 beamsplitter onto two single photon sensitive SPADs. The photon detection events on each detector are time-tagged via the time correlated single photon counting (TCSPC) electronics. The time-tagged photon arrival times are post-processed to generate the second order correlation histograms as shown in (ii). Figure 2.(ii) illustrates the fit to a low (4 μW) and high (700 μW) pump power correlation measurement, using the function in Eq.SM1. At the highest pump power, the histogram is best fit using Eq.SM1 with $\tau_1 = 0.835 \pm 0.004$ ns and $\tau_2 = 84.14 \pm 0.05$ ns. The observed bunching lifetime at high power is comparable to other emitters in wide bandgap semiconductors[1–3]. The $g^{(2)}(0)$ value as a function of the pump power in shown in (iii). Below 300 μW, $g^{(2)}(0) < 0.5$.

References

(1) Neu, E.; Agio, M.; Becher, C. Photophysics of single silicon vacancy centers in diamond: implications for single photon emission. *Opt. Express* **2012**, *20*, 19956.

(2) Kurtsiefer, C.; Mayer, S.; Zarda, P.; Weinfurter, H. Stable solid-state source of single photons. *Phys. Rev. Lett.* **2000**, *85*, 290–293.

(3) Berhane, A. M.; Jeong, K. Y.; Bradac, C.; Walsh, M.; Englund, D.; Toth, M.; Aharonovich, I. Photophysics of GaN single-photon emitters in the visible spectral range. *Phys. Rev. B* **2018**, *97*, 165202.